

Chapter 10

Structural and Functional Analyses of Bryophyte Canopies

Steven K. Rice*

*Department of Biological Sciences, Union College,
Schenectady, NY 12308, USA*

David T. Hanson

*Department of Biology, University of New Mexico,
Albuquerque, NM 87131, USA*

Zach Portman

*Department of Biology, Utah State University,
Logan, UT 84322, USA*

Summary	173
I. Introduction.....	174
II. Chlorophyll Fluorescence 2D Imaging in <i>Sphagnum</i>	175
A. Photosynthetic Drying and Light Response Curves	175
B. Fine- and Coarse-Scale Patterns of Electron Transport Rate	177
III. 3D Thermal Mapping of Bryophyte Canopies.....	178
A. Combining Thermal Imaging and 3D Laser Scanning.....	178
B. Temperature Distribution in <i>Polytrichum commune</i> Canopies.....	179
IV. Light Dynamics in Virtual <i>Bazzania trilobata</i> Canopies.....	180
A. The Plant Model	181
B. Simulating Light Within the Canopy.....	182
V. Conclusions.....	183
Acknowledgements	184
References	184

Summary

Although not often discrete, the canopy (i.e., the organization of branches, shoot systems and their extent) remains the most definable and useful unit of function in bryophytes. Chambers used for gas exchange provide an integrated summary of canopy photosynthetic function. However, other techniques can provide more information on spatial variation in physiological process in both the horizontal and vertical planes. Three examples of such studies are presented here. First, variation in photosystem II (PSII) function has been evaluated, along a canopy

*Author for correspondence, e-mail: rices@union.edu

surface, using an imaging chlorophyll fluorometer. We evaluated the quantum yield of PSII, ϕ_{PSII} , and calculated the relative rate of photosynthetic electron transport (RETR) on 7 cm diameter samples of ten *Sphagnum* species during drying. Spatial variation in RETR increased both during drying as well as in high light, which led to different relationships between mean RETR and its variation—across light gradients, the relationship was positive, but negative when RETR was reduced by tissue desiccation. Studies of photosynthetic function using chlorophyll fluorescence measurements need to match their sampling protocols to account for this difference. Further, combining a laser scanning approach that provides three-dimensional information on canopy structure with functional imaging allows assessment of function in three dimensions (3D) within the canopy. This is illustrated using a thermal imaging camera to measure temperature distribution within *Pleurozium schreberi* canopies under still conditions and with wind. This imaging system resolved 9 °C temperature differences within the canopy and localized shoot temperature relative to canopy height. Finally, computational canopy (i.e., virtual) models have been developed for bryophyte canopies, particularly ones with simple branching structure. A model of this type is shown here for the liverwort *Bazzania trilobata* and a light model implemented using a ray tracing algorithm. Output from this model followed the attenuation of light predicted by the Lambert-Beer Law and such a technique can be used to evaluate how branching architecture and density affect the dynamics of light capture in bryophytes. New approaches based on novel imaging technologies are in rapid development and present opportunities to further our understanding of function within bryophyte canopies.

I. Introduction

The canopy represents an important unit of matter and energy exchange in bryophytes; however, canopies do not display homogeneous function in either the horizontal or

vertical planes. For example, plant water status, photosynthetic pigment concentration, photosynthetic capacity, photoinhibition, leaf or shoot area, light intensity, temperature and humidity can all vary along and within bryophyte canopies (Hayward and Clymo 1982; van der Hoeven et al. 1993; Gerdol et al. 1994; Davey and Ellis-Evans 1996; Zona et al. 2011), and affect rates of whole canopy photosynthesis (Zotz and Kahler 2007; Rice et al. 2008, 2011b; Tobias and Niinemets 2010). Unfortunately, this variation is normally neglected as methods of evaluating photosynthetic function often either provide measurements of average, coarse-scale properties (>4 cm scale or above the size of individual shoots; e.g., gas exchange methods) or they allow for fine-scale measurements (0.1–2 cm or at scale of large leaves or branches; e.g., fiber-optic evaluations of chlorophyll fluorescence parameters) that may obscure larger scale patterns. Although limitations of the latter may be overcome by dense sampling and exploring the variance structure of the data,

Abbreviations: Chl – Chlorophyll; ETR – Rate of photosynthetic electron transport as calculated from chlorophyll *a* fluorescence measurements; F_0 – Baseline fluorescence in dark-adapted tissue; F_0' – Baseline fluorescence in light-adapted tissue; F_m – Maximum chlorophyll *a* fluorescence in dark-adapted tissue at saturating light; F_v/F_m – Ratio of variable ($=F_m - F_0$) to maximal fluorescence in dark-adapted tissue; F_v'/F_m' – Ratio of variable to maximal fluorescence in light-adapted tissue; I_0 – Intensity of incident light at top of canopy; I_x – Intensity of incident light at depth *x* within canopy; *K* – Light extinction coefficient; K_{app} – Apparent light extinction coefficient, product of *K* and SAI_{*x*}; PPF_D – Photosynthetic photon flux density; PRI – Photochemical reflectance index; Q_{10} – Temperature coefficient; RETR – Relative rate of (calculated) photosynthetic electron transport; SAI_{*x*} – Shoot area index above depth *x* within canopy; ϕ_{PSII} – Quantum yield of photosynthesis as calculated from chlorophyll *a* fluorescence parameters

this is rarely done. Few methods have been developed that allow investigations across fine- and coarse-scales that would help provide an understanding of how physiological processes integrate across these scales within canopies and would allow for a more mechanistic understanding of physiological scaling of bryophytes.

Consequently, we have limited understanding of how variation in the horizontal and vertical dimensions affects bryophyte canopy function. Variation in the horizontal plane will be caused by extrinsic factors that affect microclimate, particularly those influencing energy and water budgets, as well as structural variation within the canopy that affect boundary layer processes and, hence water relations, or self-shading. When integration among adjacent shoots within the canopy is limited, portions of the canopy may experience different physiological conditions. This may be caused by uneven drying, or heating because of the resistance to capillary transport and heat movement within and among shoots. Depending on the scale of the underlying causes of spatial variation and the degree of spatial integration, physiological function may vary at fine- or coarse-scales, both, or neither. Fine-scale variation may occur when biotic or abiotic conditions vary among nearby leaves or shoots when there is limited physiological integration. For example when distal leaves or branches dry, there may be limited ability for plants to rehydrate from interior water stores causing high variability in the water status of distal branches.

Coarse-scale patterns may occur when local conditions within leaves and shoots are similar, but are patchy at larger spatial scales. This can be caused by development of different heights of shoot systems, existence of capillary networks that share water among nearby, but not distant shoots, proximity to local windshelters or regions of high humidity, or to the patchy distribution of ambient light. Recent studies of spatial variation in vascular plant leaf photosynthesis using 2D imaging chlorophyll fluorometers have localized regions of high photosynthetic activity or damage

and related it to stomatal dynamics when combined with other imaging approaches (Oxborough 2004; Aldea et al. 2006; Chaerle et al. 2007; Morison and Lawson 2007; Baker 2008). In this chapter, we employ a similar approach to compare the structure of variation in photosynthetic electron transport, as inferred from chlorophyll a fluorescence measurements, during drying and across gradients of light availability in a multispecies comparison in *Sphagnum*. In addition, we introduce two methods that could prove promising for understanding physiological function and integration in studies of bryophyte canopies, namely 3D functional imaging combining laser scanning with thermal imaging and the use of simulated virtual canopies where processes can be explored using computer simulation modeling on 3D canopy representations.

II. Chlorophyll Fluorescence 2D Imaging in *Sphagnum*

Understanding the physiological mechanisms that underlie variation in whole plant or canopy function will require not only the ability to evaluate the performance of physiological units (e.g., leaves, branch systems or populations), but also variation in those units and their interaction. Using an imaging chlorophyll fluorometer (Fluorocam, PSI, Czech Republic) with a closed-chamber gas exchange system (LI-COR 6200, Lincoln, NB, USA), we have explored variation in photosynthetic characteristics obtained using chlorophyll fluorescence and CO₂ uptake simultaneously in a multi-species comparison in the genus *Sphagnum*.

A. Photosynthetic Drying and Light Response Curves

Samples of ten *Sphagnum* species that varied in their preferred habitat and morphology were collected in the field and reared in a greenhouse under 300 $\mu\text{mol quanta m}^{-2} \text{s}^{-1}$ maximum photosynthetic photon flux density (PPFD) for over 90 days. Intact 7.5 cm

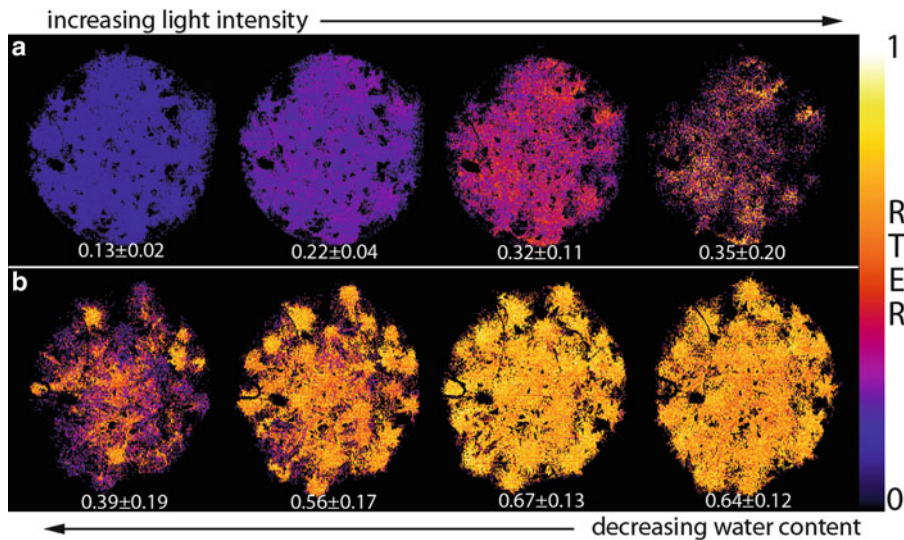


Fig. 10.1. Relative photosynthetic electron transport rates (RETR), as estimated from chlorophyll fluorescence measurements, at different water contents and light intensities in *Sphagnum recurvum* for 7.5 cm diameter samples. The quantum yield of Photosystem II, ϕ_{PSII} , as estimated from chlorophyll fluorescence parameters was measured at 0.3 mm resolution using 2D imaging. RETR was standardized relative to the maximum value in (a) during increasing light intensities (PPFD 60, 120, 250 and 500 $\mu\text{mol photons m}^{-2} \text{s}^{-1}$) and (b) during drying from optimal water content to zero. Mean RETR and standard deviations are shown. Higher RETR values and associated rates of photosynthesis at high light show elevated variation as evidenced by the increase in the standard deviation. The opposite relationship is shown when RETR was decreased during drying: where lower RETR is associated with high variation.

diameter canopies containing only new growth were used for analysis. Samples were placed in a 1.8 l closed chamber and CO_2 exchange measured in two 20 s intervals. Rates of net photosynthesis were assessed over a set of seven light intensities (30–730 $\mu\text{mol quanta m}^{-2} \text{s}^{-1}$ PPFD) for each sample ($n=3$ per species). A photosynthetic drying curve ($n=1$ per species) was also performed over a 2–3 days period. Details on sample collection, growth conditions and gas exchange are reported more fully in Rice et al. (2008). Following gas exchange measurements, a 2D imaging fluorometer (Fluorcam, PSI, The Czech Republic) was used to estimate both the photochemical yield (ϕ_{PSII}) and the relative rate of photochemical electron transport (RETR; rate of electron transport scaled between 0 and 1 for each sample) at 0.3 mm spatial scales (Fig. 10.1; for basics on chlorophyll *a* fluorescence, see Govindjee 2004; and other chapters in Papageorgiou and Govindjee (eds) 2004). LED panel lighting provided

measuring light at 618 nm and a white saturating burst. The parameter ϕ_{PSII} was calculated as Fv'/Fm' (ratio of variable to maximum fluorescence in light adapted tissue) and ETR calculated as the product of ϕ_{PSII} , the light level and 0.5, the latter to account for energy going to photosystem II (Maxwell and Johnson 2000); absorption was assumed constant among species. This may deviate from 0.5 due to system state changes (see Papageorgiou and Govindjee 2011) and we report relative rates (RETR) to account for possible variation among species. The mean and standard deviation of RETR were derived and compared.

All samples showed characteristic light response curves with light compensation points varying between 37 and 72 $\mu\text{mol quanta m}^{-2} \text{s}^{-1}$ PPFD and $\text{PPFD}_{95\%}$ (light level at 95% of maximum net photosynthesis) between 491 and 648 $\mu\text{mol quanta m}^{-2} \text{s}^{-1}$ PPFD (Rice et al. 2008). Within species, integrated values of ϕ_{PSII} and RETR showed typical

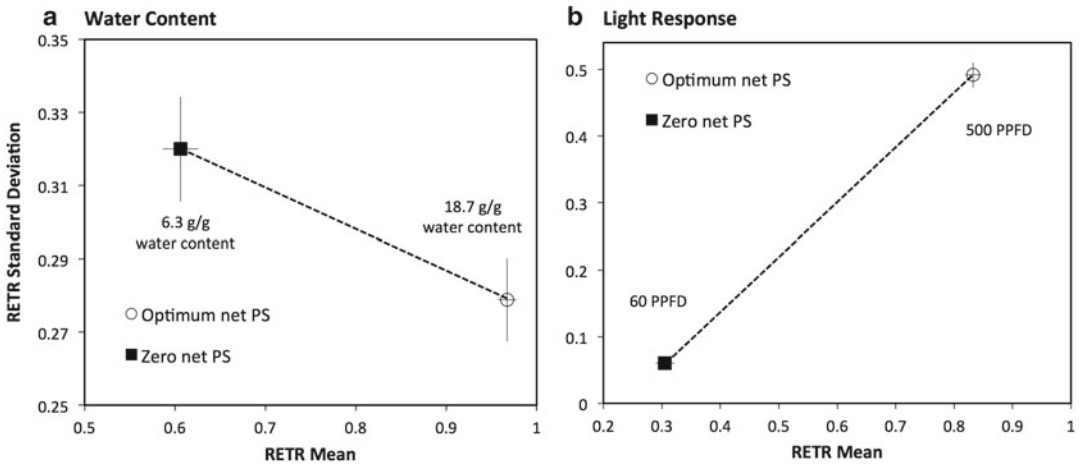


Fig. 10.2. Summary of spatial variation in relative rates of electron transport (*RETR*) estimated from imaging chlorophyll fluorescence associated with differences in plant water content (a) and light intensity (b). Means and standard errors are shown for $n=10$ samples, each of a different *Sphagnum* species. Measurements of *RETR* assume constant fraction of excited electrons going to photosystem II within a sample (Note the difference in scales).

patterns with all displaying saturating responses through $730 \mu\text{mol quanta m}^{-2} \text{s}^{-1}$ PPFD. All species sampled showed characteristic responses of net photosynthesis and *RETR* to drying. At high water content, external water films reduce access to CO_2 by increasing diffusion resistance thereby lowering rates of photosynthesis. Photosynthesis is optimized at intermediate water content where externally held water is minimized, but cells remain in full turgor. This is achieved at water content between 10 and 22 $\text{g H}_2\text{O g}^{-1}$ dry wt for the different species in this study. As plants dry, photosynthesis declines as cells desiccate. These responses were evident in the measures of net photosynthesis and *RETR*.

B. Fine- and Coarse-Scale Patterns of Electron Transport Rate

In the configuration used in this study, imaging fluorescence provides 0.3 mm spatial resolution of photosynthetic function for up to 50,000 points. This allows an evaluation of the variation as well as the spatial structure of the photosynthetic parameters. Mean and variation in *RETR* differed across both light and water content gradients (Fig. 10.1).

During light response curves, both mean values and the variation, as represented by the standard deviation of *RETR*, increased at higher light intensities and correspondingly higher rates of net photosynthesis were obtained using gas exchange (Fig. 10.2). Increased dispersion of the measurements at high light is likely caused by enhanced sensitivity to noise in calculating the ratio F_v'/F_m' , used to estimate *RETR*. The numerator, the difference between the maximum fluorescence (F_m') at the saturating burst and the minimum at ambient light (F_0'), is more sensitive to small changes in F_m' when F_0' is high under higher ambient light. Consequently, instead of indicating differences in the physiological function at fine spatial scales, higher spatial variation in *RETR* at high light is associated with greater measurement error.

In contrast, the relationship between variation and the mean *RETR* is reversed during drying (Fig. 10.1). In this case, as plants dehydrate and rates of photosynthesis and mean *RETR* decrease, the standard deviation of *RETR* increases (Fig. 10.2). During drying in *Sphagnum*, isolated distal branches, branch tips, and the edges of colonies dry first while areas of high branch and leaf density like the capitula retain water. This can

be observed in Fig. 10.1 and was common in other samples as well. This leads to spatial variation in physiological function and measures of RETR. Aggregation of regions of high photosynthetic activity increases at intermediate states of desiccation, as canopies continue to dry, the entire surface becomes desiccated and the regions of high activity become more dispersed. The cause of this pattern differs from that responsible for spatial variation in high light. During drying, high spatial variation in RETR is associated with uneven drying; it reflects underlying biophysical changes in the distribution of plant water. The large and non-uniform spatial variation observed in RETR derived from chlorophyll fluorescence studies should allow us to plan for sampling and measuring strategies in chlorophyll fluorescence studies of bryophytes. When fiber-optic probes are used, sufficient sampling should be performed to summarize variation as well as mean values.

III. 3D Thermal Mapping of Bryophyte Canopies

As the previous section illustrates, imaging systems are able to evaluate physiological function in two dimensions. Similarly, camera systems have been deployed in the field to monitor the physiological state of *Tortula princeps* (= *Syntrichia princeps*) during wet-dry cycles (Graham et al. 2006). With the development of new indices based on spectral reflectance data in the visible and near-infrared spectrum, there is now the potential to track both water status (Water Index) and physiological stress (PRI) remotely using imaging systems (Gamon et al. 1997; Lovelock and Robinson 2002; Harris 2008; Ollinger 2011). However, canopies are three-dimensional and even 2D representations will be limited in their ability to develop an understanding of canopy-level functional integration. Recent developments in 3D rendering of canopy structure using laser scanning may be combined with 2D imaging to explore physiological function in three

dimensions. Below, we provide a proof-of-concept using thermal imaging to map the temperature distribution within *Polytrichum commune* canopies.

A. Combining Thermal Imaging and 3D Laser Scanning

A 3D thermal imaging system was developed by combining a thermal imaging camera (FLIR i7, Boston, MA, USA) with 0.1 °C temperature resolution with a laser scanning system using an optical camera. In brief, the laser scanning system positions a plane of laser light perpendicular to the surface and the intersection between the canopy surface and the light is captured from the camera at an angle of 45° from the normal. Following transformation, the horizontal and vertical locations of all points along the intersection are determined. Coarse-scale patterns in canopy height were removed by using residuals from a linear multiple regression using the axes of the horizontal plane as input. Following a scan, the apparatus was moved 0.5 cm and a new scan was obtained. Ten scans allowed for the scanning of a 5 cm × 5 cm area of each sample. Details of the laser scanning system are described more fully in Rice et al. (2005). The system was constructed so that the two cameras could be positioned sequentially to view the sample from the same viewpoint, allowing for registration between images of each type. Image registration used the Turboreg plugin (Thévenaz et al. 1998) implemented in ImageJ (Abramoff et al. 2004). This brought the resolution to the minimum of the two images (120 × 120 pixels for the thermal image). Final spatial resolution was 0.23 cm/pixel in the vertical plane and 0.12 cm/pixel in the horizontal plane. After registration, images from the laser scans were thresholded to identify the portion in the laser plane and those points were selected from the thermal image. Following transformation into Cartesian spatial dimensions, the data contain spatial coordinates and temperature distribution for over 500 points within the 5 cm × 5 cm canopy (Fig. 10.3).

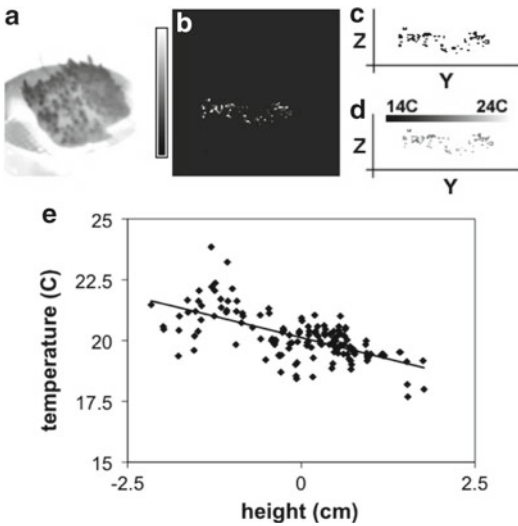


Fig. 10.3. Image acquisition and processing for 3D rendering of canopy temperatures in *Polytrichum commune*. Thermal images are taken (a) and visible light images are obtained from the same point of view. Images show intersection with the orthogonal plane of laser light (b). Images from the two sources are aligned and the laser—canopy intersection is highlighted using thresholding. The coordinates from the two images are generated following transformation (c). These points are identified in the thermal image, resulting in surface temperatures for the points within the canopy (d). Temperatures are graphed as a function of height relative to the mean canopy height (e).

B. Temperature Distribution in *Polytrichum commune* Canopies

We employed this system to explore differences in temperature distribution within canopies of *Polytrichum commune*, collected in Saratoga County, NY, USA. The stem density of the sample was 1.8 stems/cm². Samples were measured under laboratory conditions (25.5 °C, 10 % relative humidity) in still air as well as within an unconditioned flow generated by a fan (1.1 m/s average wind speed). Linear regressions were used to compare temperatures and heights within the canopy.

In still air, temperatures within the canopy ranged from 16.9 to 23.7 °C (19.9 °C mean, 1.3 °C standard deviation). With 1.1 m/s wind, temperatures were depressed and ranged from 15.2 to 23.8 °C with a 18.1 °C mean and 1.9 °C standard deviation. Under both conditions, there was a significant negative

relationship with canopy height (Fig. 10.4a, b, $p < 0.0001$); however, they differed in their slopes and also in their explanatory power. In still air, the slope of the canopy height—temperature relationship was significantly more negative (-0.76 ± 0.04) than that in wind (-0.46 ± 0.10). Without wind, the linear model accounted for 24 % of variation in the data, whereas this was only 3 % with wind.

Clearly, temperature variation within bryophyte canopies is high. Although some may be due to measurement error as there is coarse resolution of the thermal imaging system used in this study, some is clearly related to evaporative cooling within bryophyte canopies, a phenomenon expected to be greater in the upper-canopy where boundary layers are thinner. The temperature ranges displayed are biologically significant, particularly for water loss, as evaporation is a temperature-dependent process. However, they are also significant for respiratory rates as the Q_{10} (temperature coefficient) of respiration is often >2 and even above 4 in bryophytes (Davey and Rothery 1997; Uchida et al. 2002), and although photochemistry does not normally display a similarly dramatic response to temperature, Q_{10} values can also be >2 for gross photosynthesis (Davey and Rothery 1997). Canopy photosynthesis models in bryophytes have only incorporated light and shoot-level acclimation responses (Zotz and Kahler 2007; Rice et al. 2011a, b), but not temperature differences that might impact shoot-level rates of net photosynthesis. Higher temperatures that allow for increased respiration together with low light in canopy interiors would further reduce the contribution of interior shoots to net carbon gain.

The approach described above provides sufficiently resolved 3D temperature data to develop thermal models for bryophyte canopies. When combined with the biomass or shoot-area distribution within the canopy, shoot temperatures would allow development of refined canopy-level evaporation and photosynthesis models. Indeed, the degree of integration experienced by shoots and branches within the canopy, especially of plant water status, affects whole-canopy

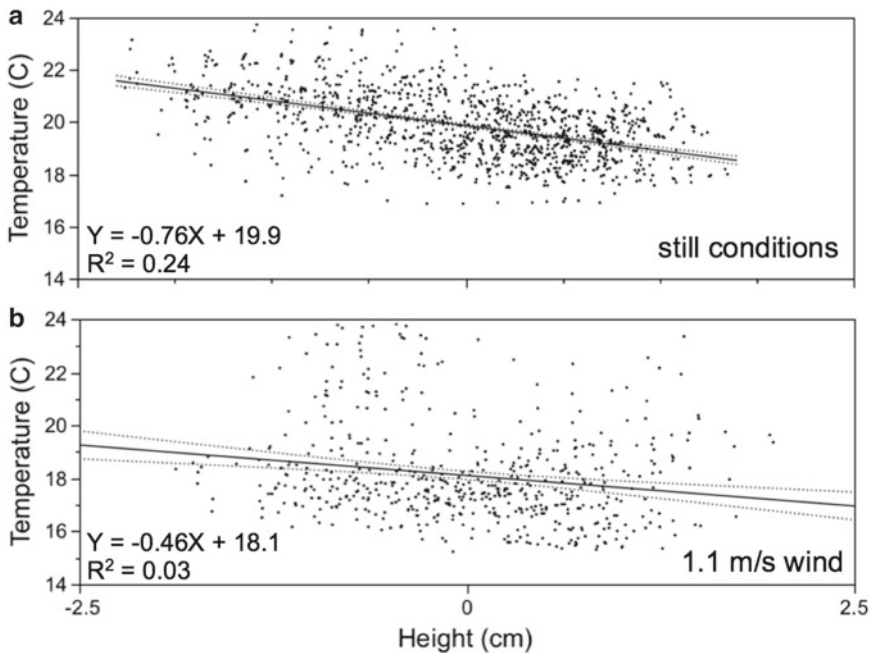


Fig. 10.4. Temperature distributions within *Polytrichum commune* canopies. Relationships are shown in still air (a) and under unconditioned 1.1 m/s wind (b) in laboratory conditions. Temperatures decline from the canopy interior to shoots that are above the mean canopy height with a more negative slope in still air (-0.76) than in wind (-0.46). Wind depressed overall temperatures and increased the variance.

function (Rice 2012) and 3D thermal imaging should allow a better understanding of this process.

In addition to thermal imaging, other imaging based physiological measurements are excellent candidates for use in 3D functional studies and include measurements of spectral reflectance to characterize indices that track water status or photosynthetic activity and 2D chlorophyll imaging systems as described in the first section of this chapter. Unfortunately, there are obstacles to developing these methods for 3D functional studies. Primarily, these approaches would be affected by changes in light intensity and/or quality within the canopy. In the case of spectral readings, reflectance from a shoot within the canopy interior is influenced by light absorption, transmission and reflection from the shoots above. Consequently, it will be difficult to determine the reflectance of the surface if the spectral quality of light falling on it is not well characterized. It might be useful to explore this problem using estimates

of average spectral signatures within the canopy; however, we would have to investigate this further to determine if there is sufficient information available here to understand the physiology of the system. Similarly, measures of chlorophyll fluorescence parameters depend on saturating pulses and given the rapid attenuation of light within bryophyte canopies, the degree of saturation may affect interpretation of the measurements. In this case, trials can be run to determine whether or not saturation has been achieved (as were performed for the section described above) and measurements performed using empirically determined, saturating conditions.

IV. Light Dynamics in Virtual *Bazzania trilobata* Canopies

Physiological function within canopies also varies in the vertical dimension, which can be caused by temperature differences described above, but also by self-shading, gradients in

plant water status, and the age and acclimation of photosynthetic tissues. Although average light attenuation profiles within bryophyte canopies appear well modeled by the Lambert-Beer Law (van der Hoeven et al. 1993; Davey and Ellis-Evans 1996; Rice et al. 2011a, b), there is high variability due to the non-uniform distribution of shoot area within the canopy. For example, in wet samples of *Andreaea depressinervis*, the coefficient of variation of local light intensity was 0.66 and 0.95 at depths of 0.5 and 1.0 cm and was higher in dry shoots (Davey and Ellis-Evans 1996).

Computer simulations have been used to create virtual canopy models and explore the interaction between plant structure and light within canopies. These methods have performed well in studies of crops, landscaped systems and forest canopies (Soler et al. 2003). Due to the complexity of light in a plant canopy, which results from the interactions of reflected, scattered, and transmitted light with individual elements (i.e., leaves, branches, shoot systems), computer simulation is a useful way to explore light dynamics. Although never employed in bryophytes, this approach can enhance our understanding of the relationship between canopy structure and the absorption and extinction of light energy. This would help us improve canopy photosynthesis models that arise from an understanding of light distributions within the canopy.

Simulating the interaction of light within plant canopies involves the intersection of two different elements: plant models and light models. The approach used in this chapter draws on the L-systems language and the PlantGL package developed by Pradal et al. (2008) from the OpenAlea software suite to create the initial plant model; it models light within the plant model using the Caribu package, also from the OpenAlea software suite.

A. The Plant Model

Lindenmayer-systems, or L-systems, were initially developed as a mathematical theory to describe plant development, but they were soon extended into a flexible plant modeling tool and remain widely used (Prusinkiewicz

and Lindenmayer 1990; Prusinkiewicz 2000). L-systems are a type of formal grammar similar to context free grammars, except all of the steps are performed in parallel. L-systems are well-suited for modeling plant development because they model the modularity and self similarity of plants in ways that mirror patterns of plant growth. The liverwort species *Bazzania trilobata* was chosen for canopy modeling due to its broad geographic range, ecological importance in boreal forests and relatively simple branching morphology, allowing it to be modeled more easily than other more structurally complex bryophytes.

Shoot structure and distributions were based on morphological measurements from 30 stems from two canopies collected in Rensselaer County, New York, USA, and measurements included: the height, width, depth, number of forks, angle of each fork, length to each fork, and length to shoot apices. The density of shoots on a ground area basis was also measured. Using morphological information, a structural model of *B. trilobata* shoots was constructed using L-systems and a canopy was simulated by populating a surface with shoots at a specified density. A custom set of L-system rules and an L-system generator were written for this project. The distribution of height, width, depth, and branch angle were incorporated into the individual shoot model using a normal distribution characterized by the means and standard deviations of the measured values. The plants were rendered using the PlantGL package of the OpenAlea software, a graphics package specializing in the visualization of plant structures.

The resulting individual morphology generated by the L-system is shown in Fig. 10.5. As the shoots grow, the lower parts senesce and these are not included in the model. Using multiple iterations of the model for individual *B. trilobata* shoots, a canopy was formed by generating plants and placing them at coordinates that matched the density of the naturally occurring specimens. Random variation was introduced along all three coordinate axes in order to produce a more realistic result. This canopy of plants was

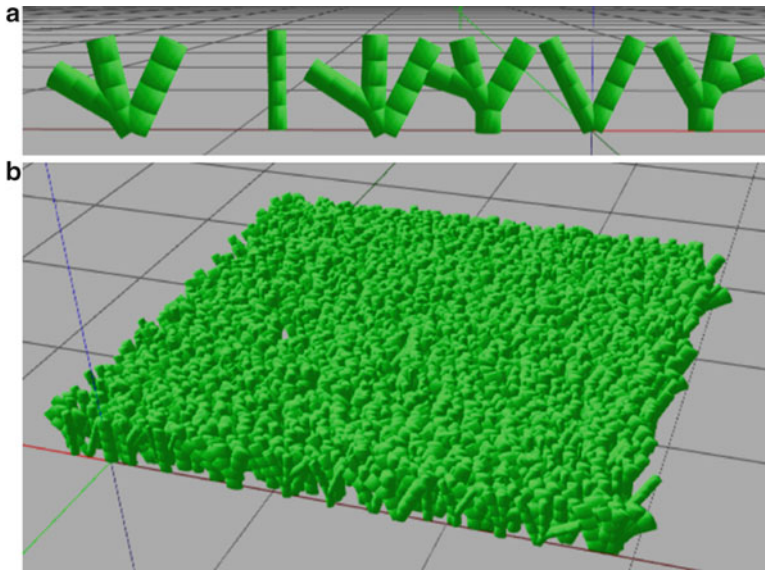


Fig. 10.5. Virtual canopy model of *Bazzania trilobata*. Some individual *B. trilobata* shoot morphologies constructed using L-systems to create individual shoots (a), which were used to populate a virtual *B. trilobata* canopy created by seeding individual shoots at natural densities (b).

then rendered using the PlantGL package. Due to the rules of the L-system used to generate the individuals, the proportion of each type of structure is the same in the computer-generated model as in the actual specimens.

B. Simulating Light Within the Canopy

Light was modeled within the canopy by the nested radiosity algorithm (Chelle and Andrieu 1998), implemented by the Caribu package of the OpenAlea software suite. The Caribu package works by modeling the light source as a diffuse mass, in this case located directly above the sample. Each individual plant that makes up the canopy is modeled as a number of discrete triangles, with potentially distinct properties of reflectiveness. The ground is also modeled and assigned its own reflectance properties. The simulation works by simulating rays of light from the source and, upon hitting each element, calculating how the light from that element affects all the other elements within a certain radius through reflectance. More sophisticated models can also incorporate transmittance, but that was not implemented in this work. For distant

elements beyond that certain radius, the original element is grouped with its neighbors and their effects are averaged together.

The Caribu simulation was performed on different modeled canopies, but the results were similar and only one is shown. The visual results of the simulation are shown in Fig. 10.6. Light attenuation for the modeled canopies followed the same general pattern that is well described by the Lambert-Beer law adapted for bryophytes: $I_x = I_o \exp(-K \cdot \text{SAI}_x)$, where I_x and I_o are the light intensities at some depth in the canopy, x , and at the surface, K is the light extinction coefficient and SAI_x is the shoot area index above point x , the surface area of shoots per ground area (cm^2/cm^2). The apparent light extinction coefficient (K_{app}) was calculated following Zotz and Kahler (2007), which is the product of K and SAI_x .

The modeled results, in comparison with measurements of light attenuation within actual canopies, displayed a much more dramatic decline in light penetration. The K_{app} was calculated for five live canopies and for five modeled canopies of the same shoot density and compared using a t-test. Mean

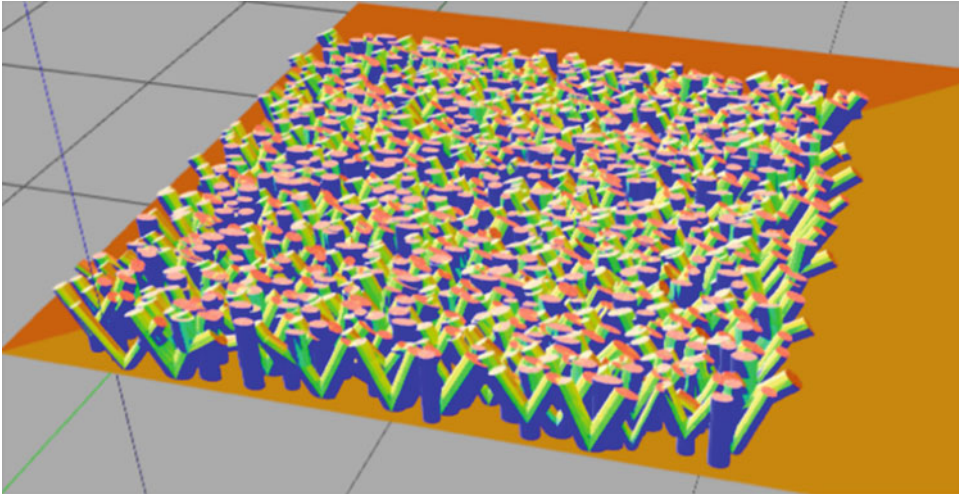


Fig. 10.6. Distribution of light within *Bazzania trilobata* canopy. A light model implementing reflected light shows the distribution of light within the canopy. Lighter colors (red, yellow) represent high light intensities and darker colors show lower intensity (green, blue).

K_{app} -value of the modeled canopies was significantly higher than the mean K_{app} -value of the actual measured canopies ($P < 0.0001$) indicating that light attenuated faster within the modeled canopies ($K_{app} = 2.7 \pm 0.1$ versus 1.3 ± 0.2 , means with standard deviations). This is likely accounted for by two factors. First, as employed, the Caribu light model only allowed reflected, but not transmitted light within the canopy interior. *Bazzania trilobata* canopies are translucent and transmitted light might penetrate more deeply within the natural canopy. Second, the orientation of the shoots is vertical and the modeled branches that record light levels within the canopy are at acute angles to direct light from above. This contrasts with a light probe, which was oriented parallel to the ground surface. Light energy distributed on a vertical surface will be reduced in intensity by a function of the sine of the angle.

Bryophyte canopy structure emerges from the interaction of leaf, branch and stem traits and experimentally determining the functional significance of variation in these traits is often compounded by lack of suitable controls. As individual traits can be manipulated independently, virtual canopy modeling may be a useful approach to understand form-function

relationships in bryophyte canopies. Further work should employ this approach to explore how variation in shoot structure affects light dynamics and incorporate the light distributions that result into a photosynthesis model to learn more about canopy-level photosynthetic processes within bryophytes.

V. Conclusions

Bryophytes present opportunities to further our understanding of canopy-level processes as whole canopies can be manipulated and evaluated by adapting techniques developed for vascular plant leaves. However, as described in this chapter, many of the traditional approaches have not allowed investigators to study functional variation in either the horizontal or vertical planes. In the simplest terms, understanding the distribution, not merely the mean values of functional traits, can help us in improving quantitative models of bryophyte canopy performance, especially when aggregation or interactions lead to non-normal distributions of functional traits. At a more complex level, these approaches will allow investigations into the physiological causes of functional variation within canopies.

For example, the capillary connection among shoots within a canopy varies among species and likely has important functional consequences. In many wet species, distal branches are often observed to desiccate first. Although this will reduce overall canopy photosynthesis, the dry shoots create additional boundary layer and prevent shoots in the interior from drying, allowing prolonged positive carbon uptake. This effect is only possible if capillary networks are not fully integrated. Species clearly differ in the degree of capillary integration among shoots, which is affected by the size, shape and spacing of leaves, by paraphyllia, and by shoot density and architecture. Just as our understanding of gas exchange in vascular plant leaves has improved by investigations of the spatial dynamics of stomatal control on leaf surfaces (Leinonen and Jones 2004; Chaerle et al. 2007; Morison and Lawson 2007; Rolfe and Scholes 2010), similar spatial dynamics are important features of bryophyte canopies in both principal planes, yet there has been little interest in exploring these processes. The novel approaches outlined in this chapter may help with such investigations.

Acknowledgements

The authors thank James Ross for conducting preliminary studies using 3D thermography, Mark Hooker, Kristina Streignitz for technical assistance. SKR thanks the Union College for sabbatical leave that facilitated writing of this chapter.

References

- Abramoff MD, Magalhaes PJ, Ram SJ (2004) Image processing with image. *J Biophotonics Int* 11:36–42
- Aldea M, Frank TD, DeLucia EH (2006) A method for quantitative analysis of spatially variable physiological processes across leaf surfaces. *Photosynth Res* 90:161–172
- Baker NR (2008) Chlorophyll fluorescence: a probe of photosynthesis in vivo. *Annu Rev Plant Biol* 59:89–113
- Chaerle L, Leinonen I, Jones HG, Van Der Straeten D (2007) Monitoring and screening plant populations with combined thermal and chlorophyll fluorescence imaging. *J Exp Bot* 58:773–784
- Chelle M, Andrieu B (1998) The nested radiosity model for the distribution of light within plant canopies. *Ecol Model* 111:75–91
- Davey MC, Ellis-Evans JC (1996) The influence of water content on the light climate within Antarctic mosses characterized using an optical microprobe. *J Bryol* 19:235–242
- Davey MC, Rothery P (1997) Interspecific variation in respiratory and photosynthetic parameters in Antarctic bryophytes. *New Phytol* 137:231–240
- Gamon JA, Serrano L, Surfus JS (1997) The photochemical reflectance index: an optical indicator of photosynthetic radiation use efficiency across species, functional types, and nutrient level. *Oecologia* 112:492–501
- Gerdol R, Bonora A, Poli F (1994) The vertical pattern of pigment concentrations in chloroplasts of *Sphagnum capillifolium*. *Bryologist* 97:158–161
- Govindjee (2004) Chlorophyll a fluorescence: a bit of basics and history. In: Papageorgiou GC, Govindjee (eds) *Chlorophyll a fluorescence: a signature of photosynthesis*, vol 19, *Advances in photosynthesis and respiration*. Springer, Dordrecht, pp 1–42
- Graham EA, Hamilton MP, Mishler BD, Rundel PW, Hansen MH (2006) Use of a networked digital camera to estimate net CO₂ uptake of a desiccation-tolerant moss. *Int J Plant Sci* 167:751–758
- Harris A (2008) Spectral reflectance and photosynthetic properties of *Sphagnum* mosses exposed to progressive drought. *Ecohydrology* 1:35–42
- Hayward PM, Clymo RS (1982) Profiles of water content and pore size in *Sphagnum* and peat, and their relation to peat bog ecology. *Proc Roy Soc Lond B Biol* 215:299–325
- Leinonen I, Jones HG (2004) Combining thermal and visible imagery for estimating canopy temperature and identifying plant stress. *J Exp Bot* 55:1423–1431
- Lovelock CE, Robinson SA (2002) Surface reflectance properties of Antarctic moss and their relationship to plant species, pigment composition, and photosynthetic function. *Plant Cell Environ* 25:1239–1250
- Maxwell K, Johnson GN (2000) Chlorophyll fluorescence—a practical guide. *J Exp Bot* 51:659–668
- Morison JIL, Lawson T (2007) Does lateral gas diffusion in leaves matter? *Plant Cell Environ* 30:1072–1085
- Ollinger SV (2011) Sources of variability in canopy reflectance and the convergent properties of plants. *New Phytol* 189:375–394
- Oxborough K (2004) Using chlorophyll a fluorescence imaging to monitor photosynthetic performance.

- In: Papageorgiou GC, Govindjee (eds) Chlorophyll a fluorescence: a signature of photosynthesis, vol 19, Advances in photosynthesis and respiration. Springer, Dordrecht, pp 409–428
- Papageorgiou GC, Govindjee (eds) (2004) Chlorophyll a fluorescence: a signature of photosynthesis, vol 19, Advances in photosynthesis and respiration. Springer, Dordrecht, 818 pages
- Papageorgiou GC, Govindjee (2011) Photosystem II fluorescence: slow changes – scaling from the past. *J Photochem Photobiol B Biol* 104:258–270
- Pradal C, Dufour-Kowalski S, Boudon F, Fournier C, Godin C (2008) OpenAlea: a visual programming and component-based software platform for plant modeling. *Funct Plant Biol* 25:751–760
- Prusinkiewicz P (2000) Simulation modeling of plants and plant ecosystems. *Commun ACM* 43:84–93
- Prusinkiewicz P, Lindenmayer A (1990) The algorithmic beauty of plants. Springer, New York
- Rice SK (2012) The cost of capillary integration for bryophyte canopy water and carbon dynamics. *Lindbergia* 35:53–62
- Rice SK, Gutman C, Krouglicof N (2005) Laser scanning reveals bryophyte canopy structure. *New Phytol* 166:695–704
- Rice SK, Aclander L, Hanson DT (2008) Do bryophyte shoot systems function like vascular plant leaves or canopies? Functional trait relationships in *Sphagnum* mosses (Sphagnaceae). *Am J Bot* 95:1366–1374
- Rice SK, Neal N, Mango J, Black K (2011a) Modeling bryophyte productivity across gradients of water availability using canopy form-function relationships. In: Tuba Z, Slack NG, Stark LR (eds) Bryophyte ecology and global change. Cambridge University Press, Cambridge, pp 441–457
- Rice SK, Neal N, Mango J, Black K (2011b) Relationships among shoot tissue, canopy and photosynthetic characteristics in the feathermoss *Pleurozium schreberi*. *Bryologist* 114:367–378
- Rolfe SA, Scholes JD (2010) Chlorophyll fluorescence imaging of plant-pathogen interactions. *Protoplasma* 247:163–175
- Soler C, Sillion F, Blaise F, Dereffye P (2003) An efficient instantiation algorithm for simulating radiant energy transfer in plant models. *ACM T Graphic* 22:204–233
- Thévenaz P, Ruttimann UE, Unser M (1998) A pyramid approach to subpixel registration based on intensity. *IEEE T Image Process* 7:27–41
- Tobias M, Niinemets Ü (2010) Acclimation of photosynthetic characteristics of the moss *Pleurozium schreberi* to among-habitat and within-canopy light gradients. *Plant Biol* 12:743–754
- Uchida M, Muraoka H, Nakatsubo T, Bekku Y, Ueno T, Kanda H, Koizumi H (2002) Net photosynthesis, respiration, and production of the moss *Sanionia uncinata* on a glacier foreland in the high Arctic, Ny-Ålesund, Svalbard. *Arct Antarct Alp Res* 34:287–292
- Van der Hoeven EC, Huynen CII, During HJ (1993) Vertical profiles of biomass, light intercepting area and light intensity in chalk grassland mosses. *J Hattori Bot Lab* 74:261–270
- Zona D, Oechel WC, Richards JH, Hastings S, Kopetz I, Ikawa H, Oberbauer S (2011) Light-stress avoidance mechanisms in a *Sphagnum*-dominated wet coastal Arctic tundra ecosystem in Alaska. *Ecology* 92:633–644
- Zotz G, Kahler H (2007) A moss “canopy” – Small-scale differences in microclimate and physiological traits in *Tortula ruralis*. *Flora* 202:661–666